Voyager Disk-Integrated Photometry of Triton

J. HILLIER, P. HELFENSTEIN, A. VERBISCER, J. VEVERKA, R. H. BROWN, J. GOGUEN, T. V. JOHNSON

Hapke's photometric model has been combined with a plane-parallel thin atmospheric haze model to describe Voyager whole-disk observations of Triton, in the violet (0.41 μm), blue (0.48 μm), and green (0.56 μm) wavelength bands, in order to obtain estimates of Triton's geometric albedo, phase integral, and Bond albedo. Phase angle coverage in these filters ranging from ~12° to 159° was obtained by combining narrow- and wide-angle camera images. An upturn in the data at the highest phase angles observed can be explained by including scattering in a thin atmospheric haze layer with optical depths systematically decreasing with wavelength from ~0.06 in the violet to 0.03 for the green filter data. The geometric albedo, phase integral, and spherical albedo of Triton in each filter corresponding to our best fit Hapke parameters yield an estimated Bond albedo of 0.82 ± 0.05. If the 14-μbar N_2 atmosphere detected by Voyager is in vapor equilibrium with the surface (therefore implying a surface temperature of 37.5 K), our Bond albedo implies a surface emissivity of 0.59 ± 0.16.

PRELIMINARY ANALYSIS OF DISK-INTEGRATED photometry of Triton based on Voyager 2 imaging data has been published by Smith *et al.* (*1*). In that report, Hapke's photometric model (*2–4*) was fit to Voyager disk-integrated data. The model fits adequately the low phase angle data ($\alpha < 139°$), but cannot model the upturn in the phase curve seen in the data at the highest phase angles observed ($139° < \alpha < 159°$; see Fig. 1). Smith *et al.* noted that this deviation is a signature of atmospheric scattering which would be greatest at high phase angles and shorter wavelengths. In this report, we fit the Voyager whole-disk data at three wavelengths to a model which includes scattering from a surface (assumed to scatter light according to Hapke's photometric model) overlain by an optically thin atmosphere haze layer in order to find a more accurate fit to Triton's phase curve and therefore obtain a better determination of Triton's geometric albedo, phase integral, and bolometric Bond albedo. Further, the surface emissivity is estimated from the bolometric Bond albedo and the inferred surface temperature.

Our analysis is based on 61 Voyager whole-disk images of Triton made with the green (0.56 μm), blue (0.48 μm), and violet (0.41 μm) filters. Suitable Voyager narrow-angle camera data exist at small phase angles (~12° to 38°) in all three filters as well as at ~133° in the green and violet bands. The phase angle coverage was extended to ~159° by using wide-angle images in all three filters. The narrow- and wide-angle cameras have been calibrated against one another using images of the Voyager calibration target taken under identical illumination conditions by both cameras. A correction for the phase curve's wavelength dependence at large phase angles and the difference in effective wavelength between the narrow- and wide-angle camera filters was performed on the high phase angle wide-angle data: the resulting correction in the violet filter is ~ −0.05 magnitude, while the shifts in the green and blue filters are inconsequential. No correction for Triton's light curve has been made; however, it is small in magnitude and would have only a negligible effect on our data.

Our haze model is based on van Blerkom's approximation to Chandrasekhar's "planetary problem" (*5, 6*). The haze, assumed to be optically thin, is characterized by an optical depth, τ_H, and a scattering phase function, $p(\cos\theta)$, where θ is the scattering angle. We have assumed the haze particle's single scattering albedo to be equal to one for simplicity. A scattering albedo less than unity would lead to slightly greater optical depths. The phase function is represented by a one-term Henyey-Greenstein function described by the asymmetry parameter, $g_{\text{haze}} = \langle\cos\theta\rangle$. For the purpose of fitting disk-averaged data at these wavelengths, a simple calculation shows that Rayleigh scattering is negligible in Triton's tenuous atmosphere.

We use Hapke's photometry theory (*2–4*) to describe the photometric behavior of the solid surface. Hapke's model employs five or more parameters to describe the scattering of light from a rough particulate surface. These are the single scattering albedo of the particles, ϖ_0; the average topographic slope angle of subresolution-scale macroscopic roughness, $\bar{\theta}$; two parameters, h and B_0, which describe the angular width and amplitude, respectively, of the opposition surge; and one or more parameters to characterize the single-particle phase function. We assumed the phase function for the surface particles to be given by a one-term Henyey-Greenstein function, described by the asymmetry parameter g_{surface}. Owing to the lack of Voyager data below a phase angle of ~12°, we could not constrain the opposition surge. However, Earth-based observations (*7, 8*) of Triton indicate that Triton does not exhibit an appreciable opposition effect; therefore, we assume that Triton has no measurable opposition surge ($B_0 = 0$) and fit only ϖ_0, $\bar{\theta}$, and g_{surface}.

Because the atmosphere is thin, we can approximate the scattering by including light which has been scattered only once or twice. Letting i and ϵ be the incidence and emission angles, respectively, and $\alpha = 180° - \theta$ be the phase angle, the expression for the scattered intensity $I(i,\epsilon,\theta)$ from the combined haze + ground system is approximated by the sum of six terms. These include a term for light scattered once by the haze only

$$I_H(\mu_0,\mu,\alpha)/F = \frac{\varpi_0 p(\alpha)}{4}\,\frac{\mu_0}{\mu + \mu_0} \times [1 - e^{-\tau_H(1/\mu_0 + 1/\mu)}] \qquad (1)$$

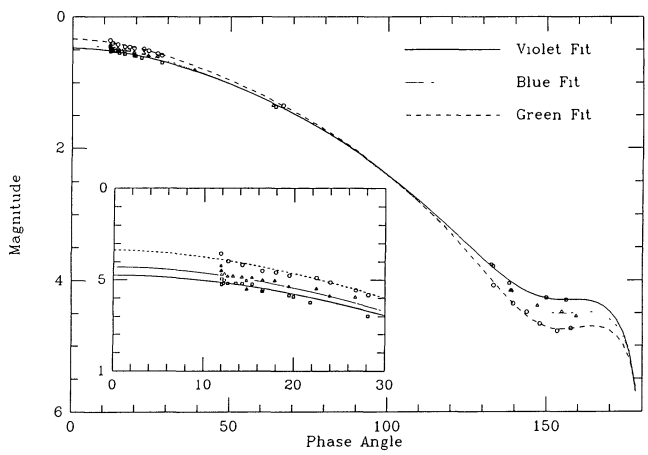

Fig. 1. Voyager violet, blue, and green filter data and our best-fit phase curves plotted on a magnitude scale. The plots are normalized such that the magnitude at zero degrees phase is −2.5 log (p), where p is the geometric albedo. For clarity, insert shows details at 0 to 30 degrees phase.

J. Hillier, P. Helfenstein, A. Verbiscer, J. Veverka, Center for Radiophysics and Space Research, Cornell University, Ithaca, NY 14853.
R. H. Brown, J. Goguen, T. V. Johnson, Jet Propulsion Laboratory, 4800 Oak Grove Drive, Pasadena, CA 91109.

A term which describes light scattered once by the surface only

$$I_G(\mu_0,\mu,\alpha)/F = I_{\mathrm{Hapke}}(\mu_0,\mu,\alpha)e^{-\tau_H(1/\mu_0 + 1/\mu)} \quad (2)$$

A term which accounts for light scattered by the haze on the way out and by the ground

$$I_{GH}(\mu_0,\mu,\alpha)/F = \frac{\varpi_0 e^{-\tau_H/\mu_0}}{4\pi}\int_0^{2\pi} d\varphi' \int_0^1 d\mu' I_{\mathrm{Hapke}}[\mu_0,\mu',\alpha'(\mu_0,\varphi_0,\mu',\varphi')] \times p(\mu',\varphi',\mu,\varphi_E)\frac{\mu'}{\mu - \mu'}(e^{-\tau_H/\mu} - e^{-\tau_H/\mu'}) \quad (3)$$

and a corresponding term for light scattered once by the haze on the way in and by the ground.

Also included is a more complex term to account for light scattered twice by the haze, and a term which accounts for light scattered by the haze which otherwise would have missed the satellite. Both of these terms are important only at large phase angles. The latter term we approximate by

$$I(\mu_0,\mu,\alpha)/F = \frac{\varpi_0}{4}p(\alpha)\left[\frac{\mu}{\tau_H}(1 - e^{-\tau_H/\mu}) - \int_0^1 e^{-(u/\mu + 2\sqrt{2ru})}du\right] \quad (4)$$

where r = (satellite radius)/(haze thickness) = 134. For a set Triton radius of 1340 km, this value corresponds to a haze thickness of 10 km (*1, 9*). We note that our results are not sensitive to the precise value of the haze thickness assumed. In the above equations, we define

$$p(\alpha) = \frac{1 - g_{\mathrm{haze}}^2}{(1 + g_{\mathrm{haze}}^2 - 2g_{\mathrm{haze}}\cos\alpha)^{3/2}} \quad (5)$$

so that

$$p(\mu,\varphi,\mu',\varphi') = \frac{1 - g_{\mathrm{haze}}^2}{[a - b\cos(\varphi - \varphi')]^{3/2}} \quad (6)$$

where

$$a = 1 + g_{\mathrm{haze}}^2 - 2g_{\mathrm{haze}}\mu\mu'$$

$$b = 2g_{\mathrm{haze}}\sqrt{1 - \mu^2}\sqrt{1 - \mu'^2} \quad (7)$$

$\varphi_0 = 0$ (assumed)

$$\varphi_E = \cos^{-1}\left[\frac{\cos(180° - \alpha) + \mu\mu_0}{\sqrt{1 - \mu^2}\sqrt{1 - \mu_0^2}}\right] \quad (8)$$

$$\alpha' = 180° - \cos^{-1}[-\mu\mu' + \sqrt{1 - \mu^2}\ \sqrt{1 - \mu'^2}\cos(\varphi - \varphi')] \quad (9)$$

Here πF is the normal incident solar flux, φ is the scattering azimuth, α is the phase angle, $\mu_0 = \cos i$, and $\mu = \cos\epsilon$. The total reflectance is given by the sum of these six terms. A plane parallel atmosphere is assumed throughout.

Table 1. Voyager 2 filter effective wavelengths and best fit Hapke and haze parameters for Triton.

Filter	Effective wavelength (μm)	Surface			Haze	
		ϖ_0	$\bar{\theta}$	g_{surf}	τ_{haze}	g_{haze}
Violet	0.414	0.995 ± 0.0005	8° ± 1°	−0.249 ± 0.024	0.06 ± 0.0025	0.65 ± 0.05
Blue	0.481	0.994 ± 0.004	10° ± 2°	−0.280 ± 0.032	0.0425 ± 0.0025	0.65 ± 0.05
Green	0.561	0.996 ± 0.003	12° ± 1°	−0.309 ± 0.010	0.03 ± 0.0025	0.65 ± 0.05

Table 2. Geometric albedos, phase integrals, and spherical albedos of Triton in the Voyager violet, blue, and green filters.

Filter	p	q	$A = pq$
Violet	0.65 ± 0.04	1.26 ± 0.03	0.81 ± 0.05
Blue	0.67 ± 0.05	1.21 ± 0.05	0.82 ± 0.07
Green	0.73 ± 0.03	1.16 ± 0.02	0.85 ± 0.03

Figure 1 shows that our model fits the detailed behavior of the phase curves at all three wavelengths. At small phase angles, Triton is brightest in the green and darkest in the violet filter, while at large phase angles, where atmospheric scattering dominates, the reverse is true. The blue filter data are intermediate to the green and violet observations. The addition of a thin atmospheric haze explains the upturn seen in the data at high phase angles well. Our best fit Hapke and haze parameters are listed in Table 1.

The surface single-particle scattering albedo of Triton (0.995) is among the highest in the solar system. Only Enceladus (0.998) and Europa (0.97) have similarly high values (*10*). The surface particles are moderately backscattering, typical of other icy satellites, perhaps slightly less so at shorter wavelengths. The haze optical depth varies roughly as λ^{-2} ranging from 0.03 in the green filter to 0.06 in the violet. The haze particles are fairly forward scattering, with $g = +0.65$, typical for haze particles seen elsewhere.

From our Hapke and haze parameters, such fundamental photometric properties as the geometric albedo, phase integral, and spherical albedo [see, for example, Veverka (*11*) for definitions] can be calculated with the results shown in Table 2. Geometric albedos vary from ~0.73 in the green to ~0.65 in the violet. For comparison, the ground-based observation by Goguen *et al.* (*7*) of $V(1,0) = -1.236 \pm 0.041$, assuming $V(\mathrm{sun}) = -26.76 \pm 0.0017$ (*12*), and a radius for Triton of 1350 km yields a visual (similar in wavelength to the Voyager green filter) geometric albedo of 0.756 ± 0.031, consistent with our green value. This agreement provides further evidence that Triton does not have an appreciable opposition surge. The phase integral is greater than unity in all three filters, which is unusual for icy, airless bodies. The large phase integrals cannot be fully explained by the forward scattering haze which only increases the phase integral a few percent. However, phase integrals greater than one might be expected for a surface covered with transparent frost grains (*13*).

Given the spherical albedo (pq), the bolometric Bond albedo can be calculated as

$$A_B = \frac{\int_0^\infty F_\odot(\lambda)A(\lambda)d\lambda}{\int_0^\infty F_\odot(\lambda)d\lambda} \quad (10)$$

where $F_\odot(\lambda)$ is the solar flux (*14*) and $A(\lambda)$ is the spherical albedo at wavelength λ. In evaluating the integrals, we have limited the wavelength range to 0.3 to 2.5 μm. The reduced solar flux outside this interval makes contributions from outside this range negligible. In the wavelength regions covered by the Voyager green, blue, and violet filters, we estimate the geometric albedos and phase integrals by a linear interpolation between the observed values at the Voyager filter effective wavelengths (Table 1). At wavelengths beyond our coverage ($\lambda > 0.56$ μm), we supplement the Voyager data with ground-based observations (*15, 16*) of the geometric albedo, as calibrated by Spencer *et al.* (*17*). However, Cruikshank *et al.* (*18*) found that the 2.3-μm methane band on Triton had become notably weaker between 1980 and 1986. Therefore, our estimates, based on the 1980 data, may underestimate the current geometric albedo, and thus the Bond albedo. The phase integral at longer wavelengths, which cannot be found from the ground-based data, is assumed to be independent of wavelength and equal to its "green filter" value of 1.16. For $\lambda < 0.41$ μm the violet spherical albedo was assumed. Integrating Eq. 10, we find a bolometric Bond albedo for Triton of 0.82 ± 0.05. The error quoted allows for a 10% error in the absolute calibration of the ground-based data by Spencer *et al.*, but does not include possible systematic errors in the absolute solar flux nor in the assumption of constant phase integral beyond 0.56 μm.

Given the Bond albedo and an estimate of the surface temperature, T, the emissivity of Triton can be determined from the energy balance equation

$$(1 - A_B)F_\odot = 4\epsilon\sigma T^4 \quad (11)$$

where $F_\odot$ is the integrated solar flux, σ is the Stefan-Boltzmann constant, and ϵ is the emissivity. Assuming a 14-μbar N_2 atmosphere in vapor equilibrium everywhere with an N_2-covered surface (therefore implying a uniform surface temperature of ~37.5 K), our Bond albedo yields a surface emissivity of 0.59 ± 0.16. The error quoted does not include possible errors in the temperature.

Our value of 0.59 for Triton's emissivity is unusually low. In comparison, almost all other satellites exhibit much higher emissivities, typically ~0.9 (*19*). A low emissivity for Triton may not be unreasonable: Triton is very cold ($T \sim 40$ K) and thus emits most of its radiation at longer wavelengths (80 to 100 μm and higher) than other solar system bodies observed to date. CH_4 and N_2 ice, both observed at Triton's surface, are relatively transparent compared to water ice, the predominant surface component on most other icy satellites [see, for example, Irvine and Pollack (*20*); Savoie and Fournier (*21*)]. Even water ice becomes significantly more transparent at Triton's longer thermal wavelengths (*20*). Therefore, the surface particles on Triton may not be as efficient emitters as those on other satellites, leading to the observed lower emissivity.

It should also be noted that we have assumed that insolation is the only significant heat source. Due to Triton's high Bond albedo and distance from the sun, its solar energy input is unusually low, and additional heat sources such as the decay of radionuclides in Triton's interior may provide additional heat on the order of 10% of the solar input (*22*), leading to a similar increase in the estimated emissivity.

REFERENCES AND NOTES

1. B. A. Smith *et al.*, *Science* **246**, 1422 (1989).
2. B. Hapke, *J. Geophys. Res.* **86**, 3039 (1981).
3. ———, *Icarus* **59**, 41 (1984).
4. ———, *ibid.* 67, 264 (1986).
5. D. J. van Blerkom, *ibid.* **14**, 235 (1971).
6. S. Chandrasekhar, *Radiative Transfer* (Dover, New York, 1961).
7. J. D. Goguen, H. B. Hammel, R. H. Brown, *Icarus* 77, 239 (1989).
8. N. L. Lark, H. B. Hammel, D. P. Cruikshank, D. J. Tholen, M. A. Rigler, *ibid.* **79**, 15 (1989).
9. G. L. Tyler *et al.*, *Science* **246**, 1466 (1989); A. L. Broadfoot *et al.*, *ibid.*, p. 1459.
10. B. J. Buratti, *Icarus* **61**, 208 (1985).
11. J. Veverka, in *Planetary Satellites*, J. Burns, Ed. (Univ. of Arizona Press, Tucson, AZ, 1977), pp. 171–209.
12. H. Campins, G. H. Rieke, M. J. Lebofsky, *Astron. J.* **90**, 896 (1985).
13. A. Verbiscer and J. Veverka, *Bull. Am. Astron. Soc.* **20**, 872 (1988).
14. Taken from J. C. Arveson, R. N. Griffin, Jr., B. D. Pearson, Jr., *Appl. Opt.* **8**, 2215 (1969).
15. D. J. Tholen, referenced in Smith *et al.* (*1*).
16. D. P. Cruikshank and J. Apt, *Icarus* **58**, 306 (1984).
17. J. R. Spencer, M. W. Buie, G. L. Bjoraker, in preparation.
18. D. P. Cruikshank, R. H. Brown, A. T. Tokunaga, R. G. Smith, J. R. Piscitelli, *Icarus* **74**, 413 (1988).
19. J. Veverka, P. Thomas, T. V. Johnson, D. Matson, K. Housen, in *Satellites*, J. A. Burns, Ed. (Univ. of Arizona Press, Tucson, AZ, 1986).
20. W. M. Irvine and J. B. Pollack, *Icarus* **8**, 324 (1968).
21. R. Savoie and R. P. Fournier, *Chem. Phys. Lett.* 7, 1 (1970).
22. R. H. Brown, *Science* **250**, 431 (1990).

23. The authors thank R. Thompson for many helpful suggestions. This research was supported by the Voyager Project and by NASA grants NSG 7156 and NAGW-2084.

9 August 1990; accepted 14 September 1990

Surface and Airborne Evidence for Plumes and Winds on Triton

C. J. HANSEN, A. S. MCEWEN, A. P. INGERSOLL, R. J. TERRILE

Aeolian features on Triton that were imaged during the Voyager Mission have been grouped. The term "aeolian feature" is broadly defined as features produced by or blown by the wind, including surface and airborne materials. Observations of the latitudinal distributions of the features probably associated with current activity (known plumes, crescent streaks, fixed terminator clouds, and limb haze with overshoot) all occur from latitude −37° to latitude −62°. Likely indicators of previous activity (dark surface streaks) occur from latitude −5° to −70°, but are most abundant from −15° to −45°, generally north of currently active features. Those indicators which give information on wind direction and speed have been measured. Wind direction is a function of altitude. The predominant direction of the surface wind streaks is found to be between 40° and 80° measured clockwise from north. The average orientation of streaks in the northeast quadrant is 59°. Winds at 1- to 3-kilometer altitude are eastward, while those at >8 kilometers blow west.

THE VOYAGER 2 SPACECRAFT ACquired a series of high-resolution images of Triton on 25 and 26 August 1989. These images showed aeolian features, such as surface wind streaks, elongated clouds, and material from active plumes being carried downwind (*1*). The ultraviolet spectrometer detected a thin atmosphere whose dominant constituent is N_2 with a CH_4 mole fraction of 2.5×10^{-6} (*2*). The atmospheric pressure was determined by the refraction of Voyager's radio signal through Triton's atmosphere to be 1.6 ± 0.3 P (*3*). Triton's near-surface temperature was determined by Voyager's ultraviolet spectrometer and infrared detector (*2, 4*) to be ~38 K. A model for sublimation-driven winds was developed subsequently (*5*) to describe Triton's atmospheric circulation.

The aeolian features (that is, features produced by or blown by the wind including surface and airborne materials) revealed in Voyager Triton images have been categorized and analyzed to gain additional insight into Triton's atmospheric dynamics. The latitudinal distribution, direction, altitude, and length have been measured. The data set used consists of a total of 16 narrow angle frames and 1 wide angle frame [see Smith *et al.* (*6*) for a description of the camera optics] with resolutions ranging from 1.4 to 81 km per line pair. These images were acquired over a period of 2 days, during which the spacecraft flew over Triton's north pole and the phase angle changed from 38° to 159° to 133°.

Aeolian features are manifested in imaging data in different ways. This report categorizes these features by their morphology and the way in which they were detected rather than by source or process although inferences will be drawn with respect to source. The classification is done this way in order to clearly establish the reliability of any particular observation. Along with surface streaks and known eruption columns, we are describing other elongated clouds, some of which appear to have fixed sources on the surface and may be other eruptions. With this approach observations of aeolian features are categorized as (i) active plumes, (ii) surface wind streaks, (iii) terminator clouds, (iv) crescent streaks, (v) limb hazes, and (vi) bright rays.

The most dramatic observations of material carried by wind in Triton's atmosphere

C. Hansen and R. Terrile, Jet Propulsion Laboratory, Pasadena, CA 91109.
A. McEwen, U.S. Geological Survey, Flagstaff, AZ 86001.
A. Ingersoll, California Institute of Technology, Pasadena, CA 91125.